Ferrous sulfide and carboxyl-functionalized ferroferric oxide incorporated PVDF-based nanocomposite membranes for simultaneous removal of highly toxic heavy-metal ions from industrial ground water

Shruti Mishra, Arun K. Singh, Jayant K. Singh*

Department of Chemical Engineering, Indian Institute of Technology Kanpur, Kanpur, 208016, India

ABSTRACT

The deterioration of the aquatic environment by the heavy metal ions contamination causes serious threat to environment and human beings. However, the treatment of complex industrial wastewater by simultaneous removal of multiple heavy metal ions via a one-step method is still extremely challenging. To this end, we synthesize ferrous sulfide (FeS) and carboxyl-functionalized ferroferric oxide (CFFO) nanoparticles, which were introduced into polyvinylidene fluoride (PVDF) matrix (individually/mixed together in an optimum ratio) through phase inversion technique. Three types of mixed matrix membranes (MMMs) were developed, viz. FeS/PVDF, CFFO/PVDF and FeS/CFFO/PVDF. The prepared membranes were characterized by SEM, TEM, AFM, FTIR, XRD, BET, and XPS techniques. The properties of the membranes were also examined for pure water flux, hydrophilicity, water uptake capacity, mechanical and thermal property, salt separation and simultaneous separation of toxic heavy metal ions such as lead, (Pb), cadmium (Cd), and chromium (Cr) from industrial ground water. The resultant membranes exhibited relatively high water flux (340–1266 L/m^{2}h) than the unmodified PVDF membrane, due to changes in the porosity and hydrophilicity of the membranes. FeS/CFFO/PVDF membrane showed that it could effectively treat Pb, Cd, Cr and As contaminated industrial ground water, simultaneously with a high removal efficiency of about 88% for Cr(VI), 99% for Cd^{2+}, 99% for Pb^{2+} and 95% for As in a single filtration process. In addition, the developed membranes conspicuously reduce their concentrations below the maximum contaminant level of WHO and BIS (India). The probable mechanism of separation of heavy metal ions through MMMs could be understood through FTIR and XPS techniques. The results of this study inferred that FeS/CFFO/PVDF membrane is a potential candidate for the simultaneous separation of Pb, Cd, Cr, and As.

1. Introduction

The demand for clean and fresh water is increasing continuously with a growing world population and socioeconomic development [1]. Due to a rapid development of global industrial activities, mining activities and energy production, the discharge of industrial wastewater from various sources are uncontrolled. This has dentrimental affects on the groundwater which is progressively contaminated with undesirable heavy metal ions [2–4]. Among the heavy metal ions Pb, Cd, Cr, As are soluble, highly toxic even at a very low concentration, mutagenic, non-biodegradable, accumulate in living organisms, and carcinogenic; thus serious threat to human health and ecological environment [2,4]. The long term consumption of drinking water contaminated with heavy metal ions can affect the renal, hematological, cardiovascular and neurological organs of the human being [5].

The simultaneous contamination of multiple heavy metal ions (Pb, Cd, Cr, As) in groundwater have been reported in different parts of India and other regions of the world [6–10]. Therefore, it is of great significance to develop effective strategies for the simultaneous separation of Pb, Cd, Cr and As from contaminated water [3].

Among various water remediation methods, the membrane filtration technology has garnered considerable attention for removal of heavy metal ions from water because of their operational simplicity, ideal for continuous flow water treatment, low energy consumption, environmental friendly nature, and manufacturing scalability [4,11]. Several different types of membranes materials, such as ceramic membranes, nanomaterial-based membrane, and mixed-matrix membranes have been reported in the literature [12]. Among them, mixed-matrix membranes (MMMs) displays a unique advantage in the separation of heavy metal ions. The MMMs are polymeric membrane

* Corresponding author.
E-mail address: jayantks@iitk.ac.in (J.K. Singh).

embedded with nanoparticles (NPs), where the separation of contaminant is controlled by the mechanisms, like, adsorption, rejection and electrostatic interaction [13,14]. The desirable properties of the MMMs like hydrophilicity, surface charge mechanical and thermal strength are governed by the embedded NPs. The effectiveness of NPs in enhancing the performance of MMMs relies on several factors like functional groups on the NPs, concentration and dispersion of NPs in the polymeric matrix.

Many types of MMMs have been previously reported for the separation of heavy metal ions from contaminated water. Liu et al. [15] used nano zero-valent iron (NZVI) blended polyacrylonitrile MMMs with the functionalization of polydopamine (PAN/PDA-NZVI) for reductive removal of Cr(VI) from the water. NZVI has a small size and larger surface area which provide higher reactivity. The resulting PAN/PDA-NZVI membrane exhibited high efficiency for Cr(VI) conversion into Cr(III). In an another study, boehmite-PVB/PVDF blended membrane-immobilized NZVI (BPPN) was synthesized via the phase inversion process for Cr (VI) removal [16]. Boehmite nanoparticles were added in the membrane to develop smoother surface with higher hydrophilicity. It was found that acidic condition was more favorable than alkaline, and reduction reaction of Cr(VI) occurred on the surface of the composite and produced precipitation of Cr (III). However, NZVI tends to agglomerate due to its high reactivity, leading to a decrease in the reduction activity. Thus, they are less likely to be suitable for long term heavy metal ion separation application. Nasir et al. [17] investigated the effect of hydrous iron-nickel-manganese trimetal oxides (HINM) NPs into polysulfone (PSF) membrane for arsenic removal from water. They found that the presence of NPs enhances the surface hydrophilicity and developed membrane can effectively treat arsenic contaminated water to reduce the concentration up to the MCL set by the WHO. Jamshidifard et al. [18]. incorporated the UiO-66-NH$_2$ MOF into the PAN/chitosan nanofibers for the removal of Pb(II), Cd(II) and Cr (VI) ions through the adsorption and membrane filtration processes. They observed that metal ions removal into the PVDF/PAN/chitosan/UiO-66-NH$_2$ nano-fibrous membrane may be controlled by inner-pores diffusion complex adsorption mechanism.

Thus, from the aforementioned studies, it can be concluded that incorporation of functionalized NPs facilitates the increase in membrane hydrophilicity and enhance the separation and removal of heavy metal ions from aqueous solution. In order to increase the hydrophilicity of the MMMs, a proper dispersion of nanomaterials with a polymeric matrix is highly desired [19]. Although above mentioned MMMs exhibited good performance, for heavy metal removal, these studies mainly focused on the separation of single pollutants from aqueous solution at a time. They did not pay much attention for simultaneous removal of multiple heavy metal ions from industrial wastewater or groundwater of industrial area. However, due to the high solubility, high migration through water flow, and atmospheric dry/wet deposition, the heavy metal ions tend to co-exist in water causing synergically higher toxicity compared to the individual ion scenario [20]. Consequently, complete aquatic system is in distress because of the presence of hazardous heavy metals either present alone or co-exist with each other [21]. Thus, it is vital to develop novel membrane materials to remove multiple heavy metals ions simultaneously from industrial effluents and real groundwater.

Therefore, keeping in view these issues, it is highly desirable to fabricate a novel nano material for MMMs with appropriate selectivity of NPs by which charge can evenly distribute on the surface of the membrane and can separate multiple heavy metal ions simultaneously. To this end, we fabricated two types of NPs, viz. Ferrous sulfide (FeS) NPs and carboxyl functionalized ferro-ferric oxide NPs (CFFO). The fabricated NPs were introduced into the polyvinylidene fluoride (PVDF) matrix (individually and mixed together in an optimum ratio) through phase inversion technique. Three types of MMMs were developed, viz. FeS/PVDF, CFFO/PVDF and FeS/CFFO/PVDF. The FeS/CFFO/PVDF MMMs were prepared using both NPs together in an optimum ratio.

Here, we have chosen PVDF as a membrane matrix because of its extraordinary properties such as excellent chemical resistance, thermal stability, high mechanical strength, good membrane-forming properties, economical and easily modifiable [22]. Despite these attractive features, PVDF matrix exhibits hydrophobicity which limits its application in long-term use for water purification system. Hence, in this study, we tried to overcome this drawback by the use of an optimum amount of FeS and CFFO NPs, and its combinations, with PVDF matrix to prepare highly selective hydrophilic MMMs.

The effect of the incorporation of individual NPs as well as synergistic effect of both NPs on the PVDF matrix was investigated in terms of physicochemical characteristics, porosity, permeability, mechanical and thermal property, and separation efficiency towards multiple hazardous heavy metal ions removal such as: Cr (VI), Cd^{2+}, and Pb^{2+} in single and mixed systems. To the best of our knowledge, FeS/PVDF, CFFO/PVDF, and FeS/CFFO/PVDF membranes have never been reported before. Hence the objective of the present study was: (i) to design and synthesize MMMs by the incorporation of FeS and CFFO NPs with PVDF matrix in an appropriate combination to improve hydrophobic property and stability of pure PVDF based membranes and use it for the separation of Cr, Cd, Pb and As from contaminated industrial ground water; (ii) to determine the properties, behaviour and mechanism of the developed MMMs (FeS/PVDF, CFFO/PVDF, and FeS/CFFO/PVDF), various characterization techniques were used. (iii) to systematically investigate the performance of the prepared membranes in terms of pure water flux, and simultaneous separation of Cr, Cd, Pb and As from the industrial ground water; (iv) to assess the salt rejection capability of the resulting membranes in the real water samples to ensure the efficiency of the membrane in practical application; (v) to investigate the interaction between metal ions and membranes.

2. Materials and methods

2.1. Materials

L-Cysteine (99%), ferric acetylacetonate (98%), sodium acrylate (98%), and dimethylacetamide (DMAc) were purchased by Merck, India. Ferric chloride, ethylenediamine, ethylene glycol, sodium acetate and other chemicals of analytical grade were purchased from Fisher Scientific, India. Polyvinylidene fluoride and polyvinylpyrrolidone (molecular weight 40000 gmol^{-1}) were purchased from Alfa-Aesar and Merck, respectively. Lead nitrate, cadmium nitrate, and potassium dichromate were procured from Loba Chemicals.

2.2. Synthesis of nanoparticles (NPs)

2.2.1. Preparation of ferrous sulfide (FeS) nanoparticles

FeS NPs were successfully prepared using the solvothermal method, which is one of the most effective and synthetic way to prepare NPs [23]. Firstly, 4 g of Ferric chloride and 1.94 g of L-Cysteine were added in 140 ml of ethylenediamine and deionized water solution of 1:1 ratio. The as-prepared mixture was stirred for 1 hour at a speed of 600 rpm to get a homogeneous solution. Subsequently, the resulting solution was transferred in a Teflon-lined stainless-steel autoclave and temperature was maintained at 200 °C for 24 h. After the complete thermal process, resultant suspended solid of FeS NPs was collected by centrifugation and washed with ethanol repeatedly until the black filtrate became colorless, and finally dried at 70 °C in a vacuum oven and stored for further experiments and characterization.

2.2.2. Preparation of carboxyl-functionalized ferroferric oxide (CFFO) nanoparticles

Solvothermal method was also used in the preparation of CFFO NPs. Briefly, 160 mL of ethylene glycol and 1.6 g ferric acetylacetonate were mixed together and sonicated for 20 min for proper dispersion. After complete dispersion, solution was stirred for 1 h at 600 rpm.

Subsequently, 3.2 g of sodium acrylate and 4 g of sodium acetate were added in a solution followed by continuous stirring for 1 hour at 600 rpm. Subsequently, resultant solution was transferred to Teflon-lined stainless-steel autoclave and kept in an oven for 24 hours at 180 °C. Then, the CFFO NPs was collected through centrifugation followed by several times washing using ethanol and then dried in a vacuum oven for 24 h at 90 °C.

2.3. Fabrication of membranes

Unmodified (PVDF membrane) and all MMMs (NPs incorporated with PVDF matrix) were prepared by using non-solvent induced phase separation method. Initially, a specific amount of NPs were dispersed in a suitable volume of DMAc solvent by ultrasonication for proper dispersion to avoid agglomeration. Next, the desired quantity of PVDF was added to the above dispersed solution along with 2 wt% of pore forming agent PVP followed by continuous stirring at 60 °C for 24 hours to obtain a homogeneous casting solution. A resultant homogeneous viscous casting solution was degassed for next 24 h to eliminate air bubbles. Then, the casting solution was dragged on a clean, and smooth glass plate as a film with a thickness of 150μm using a casting knife. After that, it was immersed into a coagulation bath containing Milli-Q water. Within a few minutes, membrane is detached from the glass plate by phase inversion process. The prepared membranes were stored in distilled water for 24 h to attain requisite mechanical strength. To improve the structure and properties of the membranes, two different types of NPs, viz. FeS and CFFO were used. By altering the concentration as well as by changing the type of NPs, different types of MMMs were synthesized. Therefore, the membranes with different compositions were designated as, FeS/PVDF, CFFO/PVDF, and FeS/CFFO/PVDF. A composition of all fabricated membranes with identification code is summarized in Table 1, and the schematic representation of the preparation of FeS/CFFO/PVDF membrane is shown in Fig. 1.

2.4. Characterization of nanoparticle's (NPs) and fabricated membranes

Zetasizer (model: Zetasizernano ZS 90), Malvern instruments, U.K., was used to analyse the particle size and distribution of NPs. To examine the morphology and structure of FeS NPs and CFFO NPs, transmission electron microscopy (TEM) analysis was carried out on a Titan G2 T-60 (FEI, Thermofisher) transmission electron microscope operated at 200 kV. Morphological images of the top surface and cross sections of the membranes were examined by field emission scanning electron microscopy (Carl Zeiss NTS GmbH, Oberkochen (Germany) Model: SUPRA 40VP). To obtain X-ray diffraction (XRD) patterns of NPs, Hecus X-Ray Systems GmbH, Graz(Austria) Model: S3 MICRO was used. The surface topology of the membranes was carried out using Atomic force microscope (AFM-Asylum Research Oxford Instrument Company, Model: MFD-3D Origin) with silicon cantilever (Model: PPN-NCLAu-10, Frequency-146-236 kHz). By analyzing the images, surface roughness was calculated and reported. To identify the presence of specific functional groups on NPs, distribution of NPs in the fabricated membranes, and to analyse chemical change occurred during filtration, FTIR spectra were recorded using FTIR spectrometer (Spectrum 100, PerkinElmer, USA) in the range of 400–4000 cm^{-1}. XPS measurements were also carried out using a PHI 5000 Versa Prob II (FEI Inc.) spectrometer using
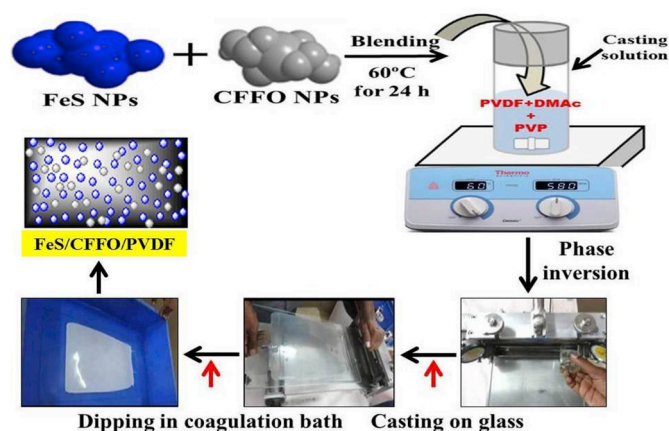

Fig. 1. Schematic illustration of the protocol used to prepare the FeS/CFFO/PVDF membrane.

non monochromatic Al Ka radiation (1486.6 eV). The surface characteristic of NPs and developed membranes namely pore size distributions (PSD), average pore radius, and specific surface were measured using an Brunauer–Emmett–Teller (BET) analyzer, Quantachrome instruments, Florida, USA (model AUTOSORB1C).

To further investigate the overall porosity of the fabricated membranes, porosity was evaluated by the gravimetric method [24]. Briefly, a sample of fabricated membranes with specific dimension (2*2 cm^2) was dipped in water for 24 h followed by wiping to remove extra water from the surface, and then weighed immediately. After weighing, samples of fabricated membranes were dried in room temperature for 24 hours and weighed again. The porosity, ε, was calculated by gravimetric method using the following equation:

$$\varepsilon = \frac{\frac{W_w - W_d}{\rho_w}}{\frac{W_w - W_d}{\rho_w} + \frac{W_d}{\rho_p}} * 100 \tag{1}$$

Where W_w is the weight of wet membrane (g), W_d is the weight of dry membrane (g), ρ_w is the density of water (0.998 g cm^{-3}), and ρ_p is the density of polymer (1.78 g cm^{-3}).

The hydrophilicity of the developed membranes was evaluated by the water uptake capacity (%) and contact angle (°) measurements. The hydrophilicity of the developed membranes were determined by the measurement of static water contact angles (WCA) using a goniometer (OCA 20, Dataphysics, Germany) by the liquid sessile drop technique using 5 μL of water as a probe liquid. Average value of five random locations was used as the contact angle to minimize the experimental errors.

Water uptake capacity (%) of each membrane was calculated using the following expression:

$$\text{Water Uptake (\%)} = \left(\frac{W_w - W_d}{W_d} \right) * 100 \tag{2}$$

Where, Ww, and W_d are the sample weights of wet and dried membranes, respectively. All measurements were repeated least three times, and the average values were reported as the water uptake (%) capacity.

Further, Breaking stress and elongation at break of the membranes

Table 1
Compositions of the casting solution for membranes and their identification code.

S. No.	Membrane code	PVDF Concentration (Wt%)	Nanoparticle conc. (Wt%)/Type	DMAC (Wt%)	PVP (Wt%)
1.	Unmodified PVDF	18	0	80	2
2.	FeS/PVDF	17	1	80	2
3.	CFFO/PVDF	17	1	80	2
4.	FeS/CFFO/PVDF	16	1:1	80	2

were measured by Universal Testing Machine, (Zwick Roell, model Z005) at a strain rate of 1 mm min^{-1} at room temperature (30 °C). Samples of membranes having dimension 2 cm × 7 cm, were analyzed. Each analysis was repeated four times to observe the reproducibility.

Thermal stability of the membranes was also examined using thermogravimetric analyser (Shimadzu, TGA-600). The experiment was carried out under nitrogen atmosphere with temperature in the range, 50–800 °C, at a heating rate of 10 °C/min.

2.5. Performance evaluation of fabricated MMMs membranes

The performance of developed membranes was evaluated using a cross flow filtration system by measuring water permeation and separation of salt and heavy metal ions. In addition, adsorption behaviour of heavy metal ions with the FeS/CFFO/PVDF membrane was also studied with batch experiments.

2.5.1. Permeation performance

Permeation performance of the developed membranes was evaluated using cross-flow filtration system unit (Sepa CF cell, Sterlitech Corp., USA) with an active membrane area of 0.0137 m$^{2.}$ Experimental set up of cross flow filtration unit is schematically depicted in Fig. S1 (Supporting information, SI). Permeation tests were performed at a constant temperature of 25 °C and constant trans-membrane pressure of 1 bar. The pure water flux of the membranes was calculated directly by measuring permeate stream in terms of liter per meter square per hour (L m^{-2} h^{-1}), as follows:

$$J_W = \frac{V}{A\Delta t} \tag{3}$$

where A is the effective membrane area (m^2), V is the permeate volume (L), and Δt is the permeation time (h).

2.5.2. Metal ion separation performance

The prepared MMMs were studied for Cr(VI), Cd^{2+}, and lead Pb^{2+} separation performance using cross-flow filtration system as used in the permeation study (Fig. S1, (SI)). The rejection of Cr(VI) was evaluated on the FeS/PVDF membrane, while rejection of cadmium (Cd^{2+}) and lead (Pb^{2+}) were examined on the CFFO/PVDF membrane. Moreover, the metal ion separation performance of the FeS/CFFO/PVDF membrane was evaluated using feed solution with metal ions, viz. Cr(VI), Cd^{2+} and Pb^{2+} having a concentration of 5 mg/L for each metal ions. This specific concentration of heavy metal ions was chosen for experiments because most of the field studies reported >5 mg/L heavy metals in contaminated surface and ground waters [27]. Neutral (6.5) and acidic pH (4.5) was used in the evaluation of separation experiments [25,26]. The experiments were performed at constant temperature of 25 °C and fixed trans membrane pressure of 1 bar. A required amount of permeate was collected at fixed time intervals. Finally the concentration of metal ions in the permeate was determined by inductive coupled plasma mass spectroscopy (ICPMS; Thermo, x-series2). Percentage rejection (% R) of metal ions were calculated using the following equation:

$$(\%R) = \left(\frac{C_f - C_p}{C_f}\right)*100 \tag{4}$$

Where C_f and C_p are the concentrations of feed and permeate, respectively. The average results of the measurements are reported in this study to minimize the errors.

2.5.3. Salt separation performance

FeS/CFFO/PVDF membrane was studied for salt separation performance using a cross-flow filtration setup as described earlier. Feed of 50 mg/L Na$_2$SO$_4$ was used as an inorganic electrolyte, to investigate the membrane potential in the rejection of sulfate ions. The concentration

of electrolyte in feed and permeate was used to evaluate the salt rejection performance (% R) by the above mentioned equation (4).

2.5.4. Adsorption isotherms

The adsorption behaviour of Cr, Cd, and Pb with the FeS/CFFO/PVDF membrane samples were studied with batch experiments. All adsorption isotherm experiments were conducted in a series of sealed conical flasks containing 0.05 g of membrane sample and 20 ml of multiple heavy metals Cr, Cd, and Pb with concentration 5, 10, 25, 50, 100, 200 and 300 mg/l. pH of the Cr solutions was maintained at pH 4.5 while Cd and Pb solution pH was maintained at pH 6.5. All solutions were kept in a shaker at 25 °C for 4 hours at 300 rpm. The residual concentrations of heavy metal were analyzed by inductive coupled plasma mass spectroscopy (ICPMS; Thermo, x-series2). The amount of solutes adsorbed was calculated by mass balance and plotted against equilibrium concentration to get the isotherm.

3. Results and discussion

3.1. Chemical and morphological characterization of NPs

The particle size distribution of FeS NPs and CFFO NPs are depicted in Fig. S2 (SI). Results showed that both NPs do not show agglomeration ensuring good dispersion property.

The transmission electron micrograph of both NPs are presented in Fig. 2(a) and Fig. 2 (b). In addition, selected area electron diffraction (SAED) patterns and lattice pattern obatained in typical HR-TEM images of CFFO NPs and FeS NPs are provided in Fig. S3 (SI) which shows good agreement with XRD data.

Fig. 2(c) shows the X-ray diffraction (XRD) patterns of NPs which identify the crystalline phases and crystalline structure of both NPs. Spectra of FeS NPs showed a main diffraction peak at around 17.1°. This observed peak corresponds to the (100) plane similar with the spectrum of typical FeS crystal [28], indicating the high crystallinity. In addition, diffraction peaks at 30.2° (220), 35.5° (311), 43.2°(400), 53.7°(422), 57.4°(511), and 62.5°(440) in the spectra of CFFO NPs attributed to the γFe$_3$O$_4$ phase (matched with JCPDS card no.(79–0417)). Thus, it is clear that the crystalline structure of the CFFO NPs did not change after the surface functionalization with the –COOH [29].

To further examine functional groups on NPs, FTIR spectra was recorded shown in Fig. 2(d). Spectra of FeS NPs possessed characteristic peaks at 535 cm^{-1} and 1037 cm^{-1}, indicating the presence of FeS NPs [30]. Moreover, spectra of CFFO NPs represented the characteristic peaks at 448 cm^{-1}, 1400 cm^{-1}, 1662 cm^{-1}, 2979 cm^{-1}, 3019 cm^{-1} and 3385 cm^{-1} assigned to the Fe–O stretching vibration, C–OH stretching vibration, C=O stretching vibration, –CH$_2$ symmetrical and –CH$_2$ asymmetrical vibration and –OH stretching vibration, respectively. These characteristic peaks confirms the functionalization of CFFO NPs by –COOH group [31].

In addition, surface area and pore size distribution of both NPs were also carried out to investigate their pore network. The surface characteristics of both NPs are listed in (Table S1 (SI)). It is evident from the data that FeS NPs used in this work possess plenty of pores with a size of 10–100 nm with a specific surface area of 7.22m^2/g. Though FeS NPs displayed a low specific surface area, it shows high removal efficiency for Cr(VI), illustrating physical adsorption was not dominant, while the reactions (Equation no. 5–7) played key role in the removal of Cr(VI). In the case of CFFO NPs, high specific surface area of 89.2 m^2/g was observed with BJH adsorption average pore size diameter of 20.2 nm. The average pore size of CFFO NPs indicate that it has mesoporous structure, and the pore acts as channel for Pb^{2+}, Cr(VI) and Cd^{2+} adsorption.

To further explore the chemical composition of developed NPs, XPS was also employed and high scan peak of Fe and S is depicted in Fig. 2(e) (f). The peaks at 165.0 eV and 710.3eV were observed corresponding to S^{2-} and Fe^{2+}, respectively. Moreover, a peak at 710 eV
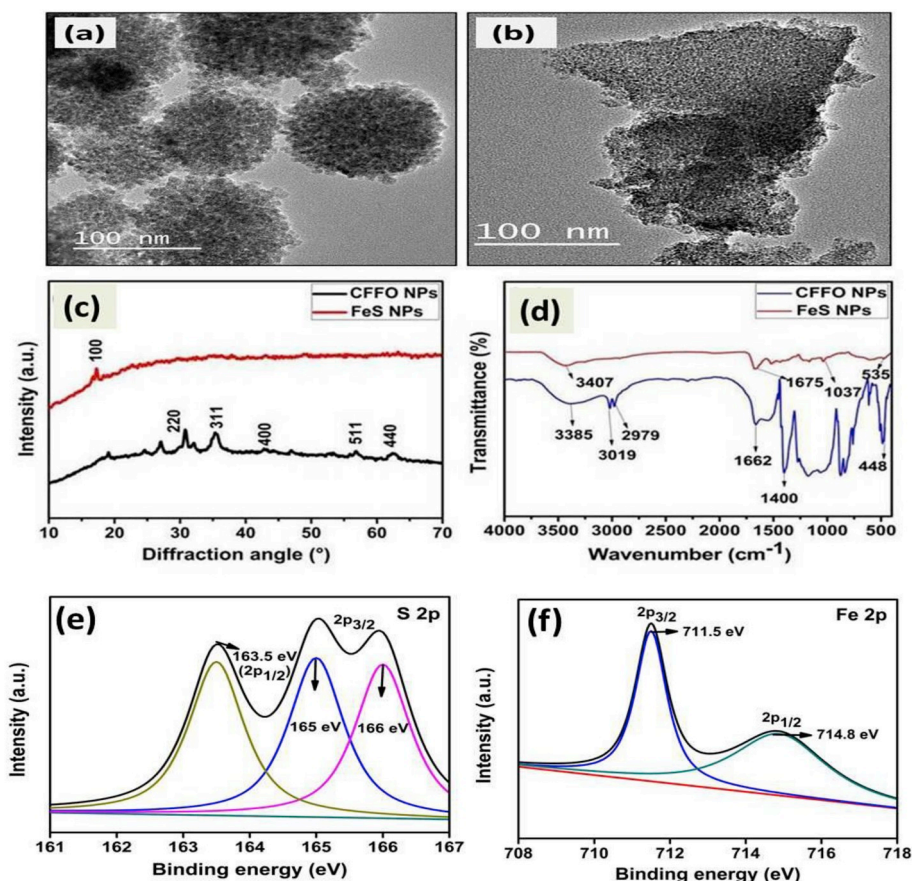
Fig. 2. Characterization of CFFO and FeS NPs: (a) TEM image of CFFO NPs (b) TEM image of FeS NPs (c) XRD pattern (d) FTIR spectra (e) High resolution scans of S 2P (f)High resultion scan of Fe 2P.

was observed in the spectra of CFFO NPs, corresponded to the presence Fe. Thus, results suggested that both Fe^{2+} and S^{2-} played key role in the reduction of Cr(VI), while binding site available on CFFO NPs played major role in the adsorption of Pb^{2+} and Cd^{2+}. Probable mechanism is discussed in the later section (Section 3.4).

3.2. Characterization of fabricated MMMs

3.2.1. SEM analysis

Fig. 3 shows the cross-section and top surface images of fabricated membranes. SEM images of the top surface of the membranes shown in Fig. 3(i)–(l), depicted absence of the agglomerated particles, which can corroborate well dispersion of the NPs. However, it has been reported that poor dispersion of NPs throughout membrane is one of the significant issue which can effect performance and mechanical strength of the membranes [32–34]. The absence of any indication of trapping or blocking of pores by NPs in cross section as well as top surface images results in the development of evenly distributed smother surface with enhanced mechanical strength. In addition, at maximum NPs concentration in FeS/CFFO/PVDF membrnae, some small pores were observed in Fig. 3(l), supporting the pore forming nature of NPs due to the presence of hydrophilic moieties, which helps to increase the mass transformation between solvent (DMAc) and nonsolvent (water) [35,36]. High degree of porosity at maximum NPs concentration was also confirmed by cross section image in Fig. 3(h). This significant enhancement in the porosity of the FeS/CFFO/PVDF membrane further confirms the effectiveness of the membrane for high water flux.

3.2.2. AFM analysis

AFM analysis was carried out to further examine the surface

morphology and two-three dimensional images of MMMs, shown in Fig. 4. Using AFM images, roughness parameters: the root mean square roughness (RMS), and the average roughness (Ra) were calculated (Table S2, (SI)). It is evident from data, that after incorporating different type of NPs, individually and combinedly in a casting solution, average roughness (Ra) of membrane surface decreased from 67.2 nm to 28.7nm. These observed decreases in surface roughness may be attributed due to increased viscosity of casting solution by increasing the amount of NPs [37]. In general, higher surface roughness has a high tendency of getting fouled leading to pore blockage [38]. Hence, it is also clear that fabricated membranes have ability to prevent the adhesion of unwanted particles on the surface due to the decrement of roughness, as shown in Fig. 4 (d), 4(f) and 4(h).

3.2.3. FTIR analysis

The FTIR spectra of unmodified PVDF membrane and MMMs (FeS/PVDF, CFFO/PVDF and FeS/CFFO/PVDF membrane) are presented in Fig. 5. The broad peaks at 2982 cm^{-1} and 3024 cm^{-1} corresponds to the –CH_2 symmetrical and –CH_2 asymmetrical vibrations, respectively in the spectra of unmodified PVDF [39]. The bands at 1423 cm^{-1}, and 840 cm^{-1} attributed to the CH_2 wagging, and C–F stretching vibration, respectively [39]. In addition, the presence of another low-intensity peak at 3406 cm^{-1} can be assigned to the O–H stretching vibration. After incorporation of FeS NPs on PVDF matrix, three peaks appeared at 3018 cm^{-1}, 2979 cm^{-1}, and 509 cm^{-1}, indicating –CH_2 symmetrical, –CH_2 asymmetrical vibrations, and presence of iron sulfide NPs, respectively [31,32]. On the other hand, spectra of CFFO/PVDF membrane possess a more intense peak of –OH group at 3424 cm^{-1} representing the enhanced hydrophilicity due to –COOH functionalization in CFFO NPs. Additionally, two peaks were found at
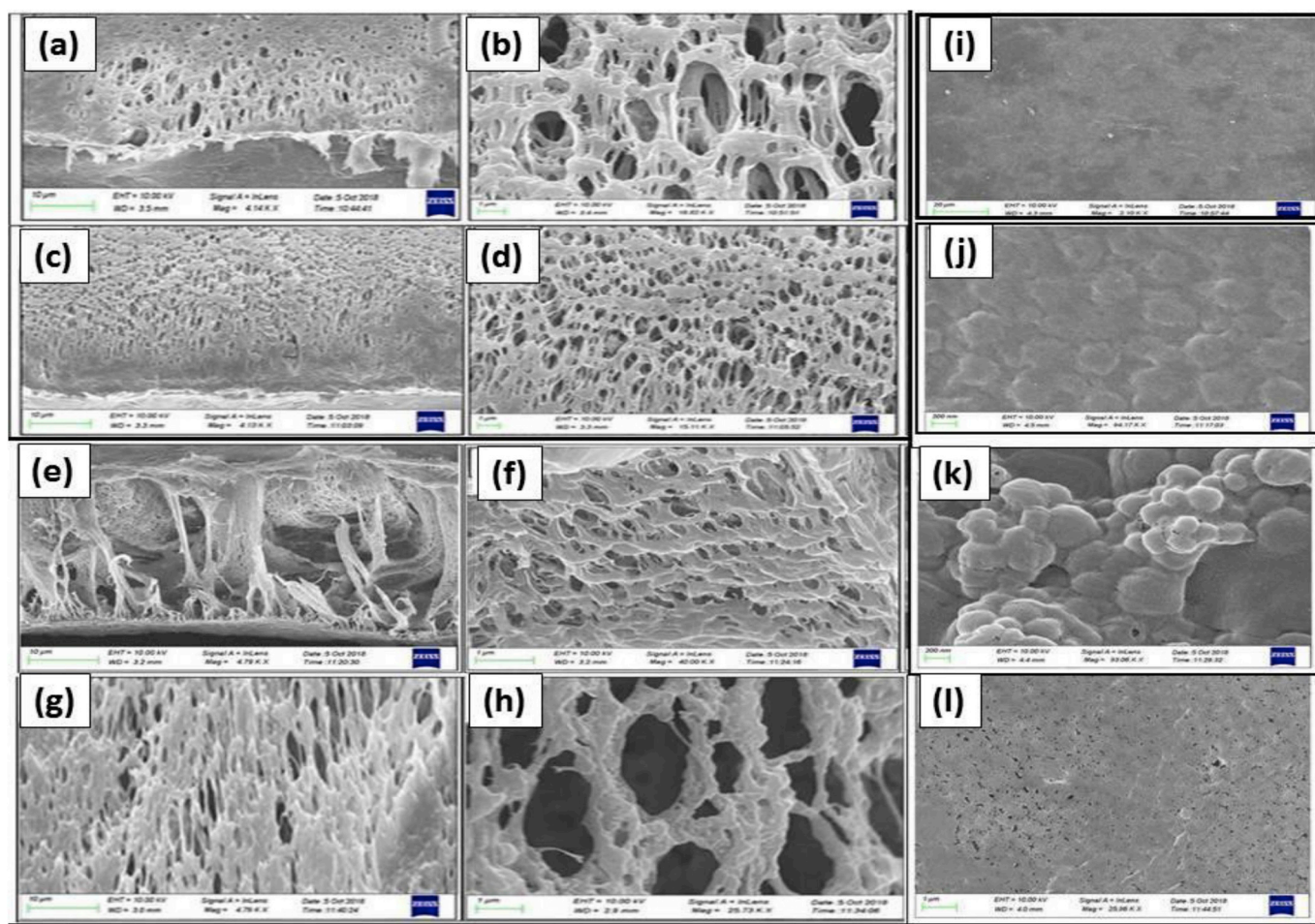
Fig. 3. SEM images of cross-sections of (a, b) Pristine PVDF; (c, d) FeS/PVDF; (e, f) CFFO/PVDF; (g, h) FeS/CFFO/PVDF with different magnification; Top surface images of (i) PVDF; (j) FeS/PVDF; (k) CFFO/PVDF; (l) FeS/CFFO/PVDF membranes.

1640 cm^{-1} and 1412 cm^{-1} corresponded to the C=O, and C–OH stretching vibration, respectively, displaying the presence of –COOH [25]. Besides, FeS/CFFO/PVDF spectra possessed characteristic peaks (2978 cm^{-1} for the –CH$_2$ symmetrical vibrations, 3018 cm^{-1} for –CH$_2$ asymmetrical vibrations, 1671 cm^{-1} for –C=O stretching vibrations, 448 cm^{-1} for FeS NPs), illustrating that both FeS and CFFO NPs distributed very well on combined NPs embedded FeS/CFFO/PVDF membrane surface.

3.2.4. Surface area, porosity, and pore size distribution analysis

To examine the effect of variation in the type and concentration of NPs on pore size distribution, BET analysis was performed. Surface characteristic of fabricated membranes are listed in Table S3(SI). It was observed that cumulative pore volume distribution of unmodified membrane is less than all the three fabricated membranes. However, both type of NPs embedded FeS/CFFO/PVDF membrane showed high cumulative pore volume distribution, indicating high porosity. Moreover, BET surface area of FeS/CFFO/PVDF was observed 20.7 m^{2}g. Which is higher than the unmodified PVDF membrane (4.5 m^{2}g). Thus, the higher pore volume and higher surface area not only enhance permeability of the membrane, also provide active binding sites for better interaction with metal ions. This observation is in agreement with the permeability, overall porosity, and SEM observations.

As can be observed in Table 2, FeS/CFFO/PVDF membrane offer greater porosity (98.8%) in comparision to other fabricated membranes. Incorporation of both types of hydrophilic NPs in an optimized ratio of 1 wt% into the polymer matrix could enhance exchange of solvent and non-solvent in the phase inversion process. Thus, voids and

cavities are formed between NPs and the polymer due to heterogeneity which increases volume of membrane leading to higher porosity of FeS/CFFO/PVDF membrane. This behavior is also reported by other researchers [23,40]. Moreover, incorporation of both types of NPs increases the thermodynamic instability of casting solution in the coagulation bath which leads to an accerated solvent and nonsolvent demixing, thus attributing to the formation of more porous structure. This results is also agreement with the BET measurement.

3.2.5. Water uptake capacity and contact angle measurement

The relative hydrophilicity of fabricated MMMs was evaluated by water contact angle (WCA°) measurements and water uptake (%) capacity. The water uptake capacity and WCA of the fabricated membranes were evaluated and results are shown in Table 2. The value of these properties generally depends on number of hydrophilic sites present on membrane surface [41]. With increase in hydrophilic sites on MMMs, water uptake capacity increases and contact angle decreases. As observed from Table 2, among all three MMMs, the FeS/CFFO/PVDF membrane showed high water uptake capacity and lower contact angle. Contact angle of unmodified PVDF membrane was found about 88.9°, representing high intrinsic hydrophobic characteristics. However, addition of hydrophilic NPs in PVDF, enhances the hydrophilicity as reflected in the decrease of contact angle viz. 72.9°, 50.2°, and 42.8° for FeS/PVDF, CFFO/PVDF, and FeS/CFFO/PVDF membranes, respectively (Fig. 6(a)). Thus it is evident from the result that incorporation of NPs increased the hydrophilic behaviour due to the presence of greater number of hydrophilic sites (-COOH and –OH) which increases the affinity of membrane towards water and enhances the diffusion of solvent
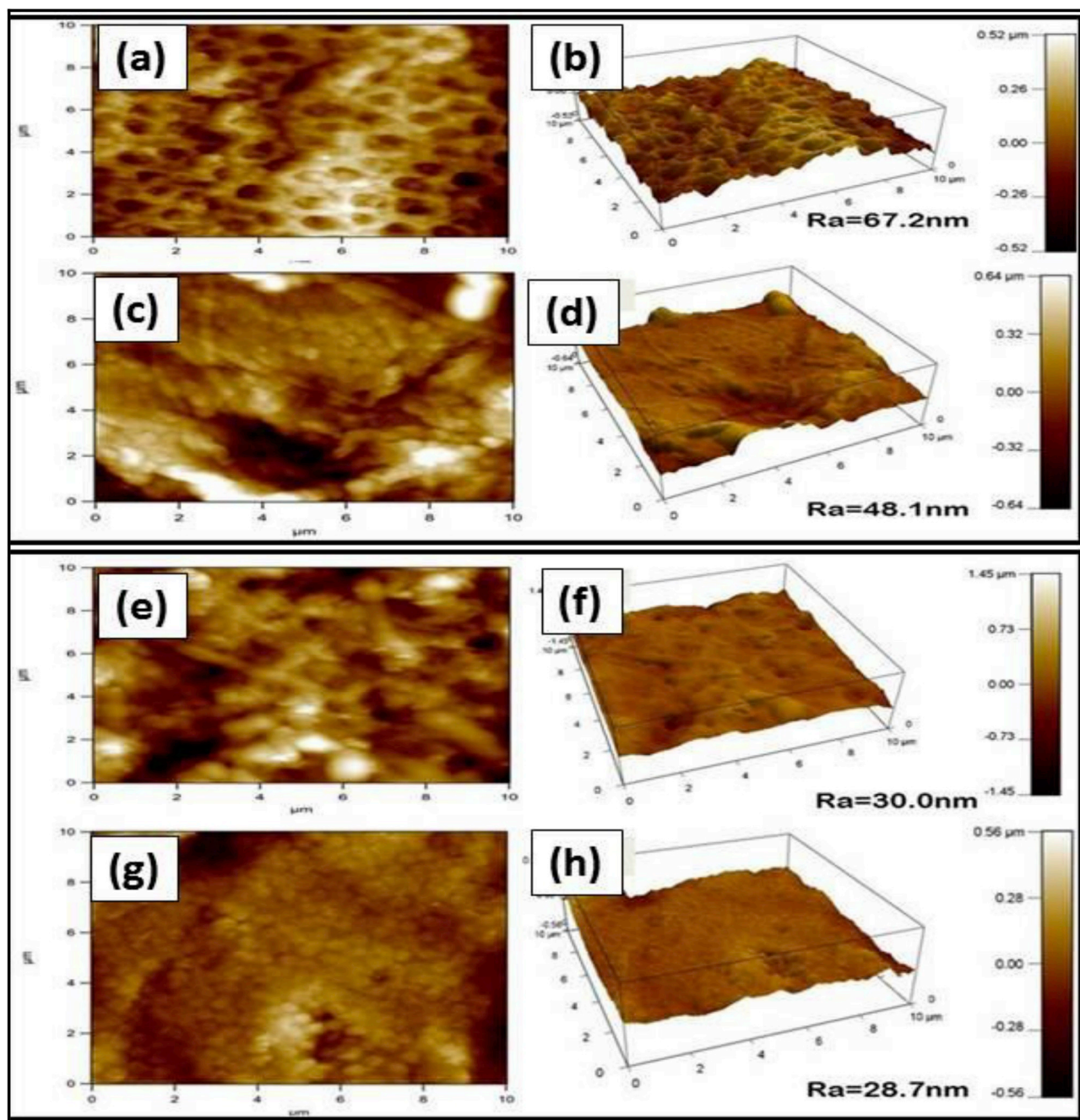
Fig. 4. 2D (left) AFM images of fabricated membranes: (a) Unmodified PVDF, (c) FES/PVDF, (e) CFFO/PVDF, (g) FeS/CFFO/PVDF, and 3D (right) AFM images of fabricated membranes: (b) Unmodified PVDF, (d) Fes/PVDF, (f) CFFO/PVDF, (h) FeS/CFFO/PVDF.

into membrane matrix by providing more spatial region [41]. This results are also agreement with roughness data (Fig. 4).

3.2.6. Mechanical and thermal stability

Variations in the breaking stress for fabricated membranes is presented in Fig. S5(a) (SI). NPs act as a bridge among polymer molecules to come closer and do not create non-uniformity. As a result, mechanical strength of MMMs is enhanced and found good mechanical strength with the increase of NPs. High breaking stress was observed for FeS/CFFO/PVDF membrane among all MMMs, indicative of a high mechanical strength (Table-2).

Fig. S5(b) (SI) shows the thermal stability of NPs modified membranes at a heating rate of 10 °C/min. It is evident from the data that although all NPs modified fabricated membranes have almost the same

shape, FeS/CFFO/PVDF membrane seem to be more stable after comparing its TGA curve with the curve of FeS/PVDF and CFFO/PVDF in the temperature range of 373–520 °C. The temperature corresponding to maximum degradation rate (Tmax) of CFFO/PVDF was observed 430.3 ± 0.5 °C and extensively increases to 487.2 ± 0.6 °C and 504.4 ± 0.6 °C for the FeS/PVDF and FeS/CFFO/PVDF, respectively. Difference between the thermal stability of FeS/CFFO/PVDF and others was about 70.1 °C. Thus, it is validated from the results that incorporation of both NPs in FeS/CFFO/PVDF induced better stability which is due to the availability of functional groups of NPs, leading to strong interfacial bonding between PVDF matrix and NPs. Thus, the starting temperature of degradation of FeS/CFFO/PVDF was higher as compared to single NPs embedded membranes. This results are well in agreement with mechanical stability.
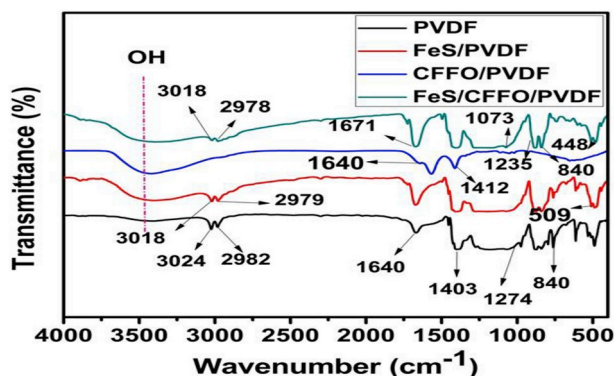
Fig. 5. FTIR spectra of unmodified PVDF, FeS/PVDF, CFFO/PVDF and FeS/CFFO/PVDF membrane.

3.3. Permeation and separation performance of fabricated membranes

3.3.1. Permeation performance

Pure water flux considered to be one of the key specification parameter for any filtration membranes. The pure water flux of fabricated membranes with respect to time are shown in Fig. S6 (SI). It is evident from Fig. 6(b) that FeS/CFFO/PVDF membrane exhibited highest flux of 1266 $Lm^{-2} h^{-1}$ than the flux 978 $Lm^{-2} h^{-1}$, 420 $Lm^{-2} h^{-1}$, 340 $Lm^{-2} h^{-1}$ of CFFO/PVDF, FeS/PVDF, and unmodified PVDF membrane, respectively. The enhanced permeability of the fabricated membranes is consistent with the water uptake, contact angle, porosity and membrane morphology parameters described above. Generally, three main factors are known to contribute the enhancement of water permeability. First, the loading of different types of hydrophilic NPs enhances the hydrophilicity of the PVDF membrane, due to the elevation of hydrogen bond interaction between water molecule and surface of membrane. Second, by the incorporation of hydrophilic NPs, the dense polymeric chains packing is disrupted introducing more free volume for water molecules passing through. Third, a thermodynamic instability is induced by the addition of hydrophilic NPs, leading to the formation of porous structure [42–44].
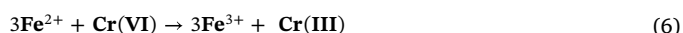
3.3.2. Metal ions separation performance in acidic and neutral pH

Metal ion separation performances of FeS/PVDF, CFFO/PVDF, and FeS/CFFO/PVDF membranes were conducted with Cr(VI), Cd^{2+} and Pb^{2+} solutions and the results are shown in Fig. 7. FeS/PVDF membrane was examined for the separation of Cr(VI) at pH 4.5 (Fig. 7(a)), while separation efficiency of CFFO/PVDF membrane was investigated towards Cd^{2+} and Pb^{2+} individually, at pH 6.5 with respect to time (Fig. 7(b)). Generally, Cr(VI), Cd^{2+} and Pb^{2+} tended to coexist in real ground water/industrial waste water due to high solubility and migration [45]. Due to their coexistence in the environment, it is essential to remove Cr(VI), Cd^{2+} and Pb^{2+} simultaneously, from the water. In order to remove Cr(VI), Cd^{2+} and Pb^{2+} ion simultaneously, performance of FeS/CFFO/PVDF membrane was evaluated in neutral (pH-6.5) as well as in acidic pH (pH-4.5) with respect to time (Fig. 7(c) and (d)).
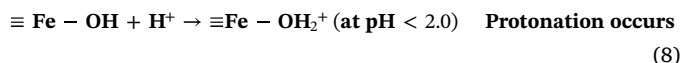
The removal performance of the fabricated membranes as depicted in Table 3, illustrated that FeS/PVDF membrane could remove

approximately 63.7–95.7% of Cr(VI) while CFFO/PVDF membrane could remove around 76.2–87.9% of Cd^{2+}, and 99.4–99.7% of Pb^{2+} from an individual aqueous solution of each. However, FeS/CFFO/PVDF membrane showed improved removal efficiency for Cr(VI), Cd^{2+} and Pb^{2+} in acidic as well as in neutral pH. The higher removal efficiency of FeS/CFFO/PVDF membrane towards all three metal ions is observed due to the combinational properties of both NPs (FeS NPs and CFFO NPs) in the MMMs.
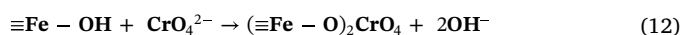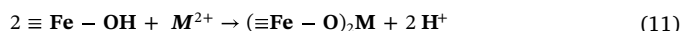
FeS NPs and CFFO NPs play an important role in selective adsorption/reduction and repulsion of heavy metals ions on each fabricated membrane [23]. The FeS NPs can efficiently separate the Cr (VI) from the contaminated water via reduction and adsorption approach [23]. Mechanism of adsorption and reduction of Cr(VI) is shown in equations (5)–(7):

$$FeS + H^+ \rightarrow Fe^{2+} + HS^- \tag{5}$$

$$3Fe^{2+} + Cr(VI) \rightarrow 3Fe^{3+} + Cr(III) \tag{6}$$

$$3S^{2-} + 2Cr(VI) \rightarrow 3S + 2Cr(III) \tag{7}$$

However, CFFO NPs consist large number of active binding sites (Fe–OH, Fe–O-) and hydrophilic –COOH and –OH moiety, responsible for more numerous interactions with metal ions [25]. With a change in pH, the neutral surface sites Fe–OH acquire (+) ve or (−)ve charge by protonation or deprotonation, respectively. The reactions are shown in equations (8) and (9):

$$\equiv Fe - OH + H^+ \rightarrow \equiv Fe - OH_2^+ \text{ (at pH} < 2.0) \quad \textbf{Protonation occurs} \tag{8}$$

$$\equiv Fe - OH \rightarrow + FeO^-$$
$$+ H^+ \qquad \text{(at pH} > 2.0) \qquad \textbf{Deprotanation occurs} \tag{9}$$

These binding sites can easily coordinates with the metal ions followed by loss of protons to form monodentate and bidentate complexes as shown in equation (10)–(12):

$$\equiv Fe - OH + M^{2+} \rightarrow \equiv Fe - OM^- + H^+ \tag{10}$$

$$2 \equiv Fe - OH + M^{2+} \rightarrow (\equiv Fe - O)_2M + 2 H^+ \tag{11}$$

$$\equiv Fe - OH + CrO_4^{2-} \rightarrow (\equiv Fe - O)_2CrO_4 + 2OH^- \tag{12}$$

Thus, above equations are agreement that combined NPs (FeS NPs and CFFO NPs) incorporated FeS/CFFO/PVDF membrane showed enhanced removal efficiency towards simultaneous removal of Cr (VI), Cd^{2+}, and Pb^{2+} in acidic as well as in neutral pH (Table 3). Moreover, higher rejection of Pb^{2+} was observed compared to Cr(VI) and Cd^{2+}. This observation may be due to the hydrated radii of Pb^{2+} than other metal ions, and the possibility of the formation of the lead complex with anion moieties leads to the enhanced rejection through size exclusion principle. In addition to the size exclusion, Pb^{2+} also gets adsorbed on the membrane surface due to the presence of negative (−) charge on the surface of the membrane at PH 6.5. Similar observation for Pb^{2+} has also been reported by other researchers [46–48].

It is evident from the results, that enhanced simultaneous rejection of all three hazardous heavy metal ions through FeS/CFFO/PVDF membrane was attributed due to the synergistic effect of both NPs, which enhances hydrophilicity, adsorption/reduction and adsorption/repulsion rate for heavy metals ions. Schematic representation of the

Table 2
The characteristic features of fabricated MMMs.

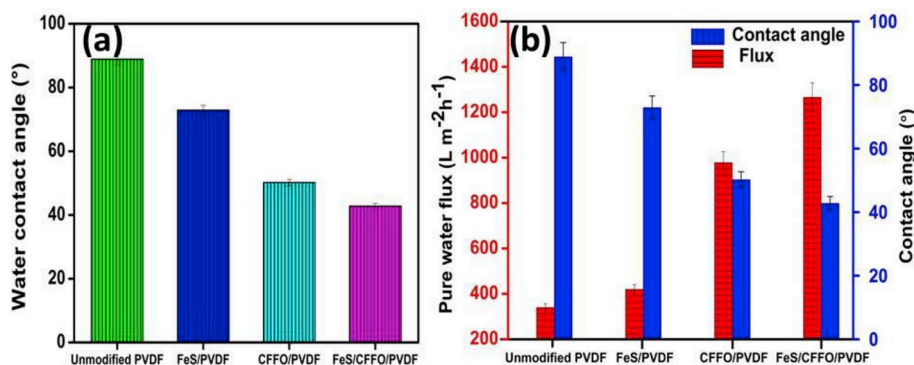| Membrane code	Water Uptake (%)	Contact angle (°)	Porosity (%)	Pure water flux (L/m²h)	Breaking Force (N)
PVDF	37.76	88.9	40.6	340	1.93
FeS/PVDF	87.4	72.9	90.2	420	2.37
CFFO/PVDF	91.2	50.2	95.4	978	2.85
FeS/CFFO/PVDF	96.7	42.8	98.8	1266	5.78

Fig. 6. (a) Water contact angle of unmodified PVDF membrane and modified membranes; (b) Change in pure water flux of fabricated membranes with respect to change in contact angles.

mechanism of combined NPs embedded highly efficient FeS/CFFO/PVDF membrane is depicted in Fig. S7 (SI), showing the role of both NPs in the fabricated membrane.

In neutral pH (6.5), active binding sites of CFFO NPs and –COOH will be present in its ionized form (FeO$^-$ and -COO$^-$), responsible for the (−)ve charge throughout the membrane. Thus, Cd^{2+} and Pb^{2+} are strongly removed through surface of the membrane due to the formation of monodentate or bidentate complexes. However, in the neutral pH Cr(VI) present in its ionic form in aqueous solution as $Cr_2O_7^{2-}$ and CrO_4^{2-} [35,49,50]. Presence of negative charge on Cr species and the surface of the membrane, leads to the Cr (VI) repulsion through surface of membrane. Therefore, the presence of charged functional groups on the membrane surface tend to repel/attract the metal ions, leading to metal ion separation.

Moreover, metal ions rejection experiments were also performed in acidic pH (4.5). In acidic pH, active binding site of CFFO NPs (Fe–OH group) will be present in the protonated form (Fe–OH$_2^+$) [51]. According to electrostatic repulsive interaction mechanism (Fig. 8), the positive charge on membrane surface enhanced, leads to the high repulsion between positively charged metal ions (Pb^{2+} and Cd^{2+}) and membrane surface. However, in the acidic medium Cr generally exist in the HCrO$_4^-$ form [52], which could be attributed to the complexation with protonated membrane surface leads to the retention of HCrO$_4^-$ on

Table 3
Hazardous heavy metal ions rejection through developed membranes.

Membrane code	Ion	Testing Conditions	Rejection (%)
FeS/PVDF	Cr(VI)	feed, 5 ppm; pH 4.5; pressure, 1 bar	63.70–95.71
CFFO/PVDF	Cd^{2+}	feed, 5 ppm; pH 6.5; pressure, 1 bar	76.2–87.9
	Pb^{2+}	feed, 5 ppm; pH 6.5; pressure, 1 bar	99.4–99.7
FeS/CFFO/PVDF	Cr(VI)	feed, 5 ppm; pH 4.5; pressure, 1 bar	82.9–88.4
	Cd^{2+}	feed, 5 ppm; pH 4.5; pressure, 1 bar	89.1–90.1
	Pb^{2+}	feed, 5 ppm; pH 4.5; pressure, 1 bar	99.8–99.0
FeS/CFFO/PVDF	Cr(VI)	feed, 5 ppm; pH 6.5; pressure, 1 bar	76.5–86.18
	Cd^{2+}	feed, 5 ppm; pH 6.5; pressure, 1 bar	95.3–99.0
	Pb^{2+}	feed, 5 ppm; pH 6.5; pressure, 1 bar	99.78–99.1

Besides, FeS/CFFO/PVDF membrane performance towards the simultaneous separation of multiple ions in acidic as well as in neutral pH can also be explained as follows.

the membrane surface.

Hence it is manifest from the results, that FeS/CFFO/PVDF membrane is highly efficient to removal multiple heavy metals ions simultaneously from both acidic as well as in neutral environmental conditions due to the combination of Donnan and size exclusion principle. Besides, to explore the adsorption capacity of FeS/CFFO/PVDF towards heavy metals ions, batch experiments were also performed.
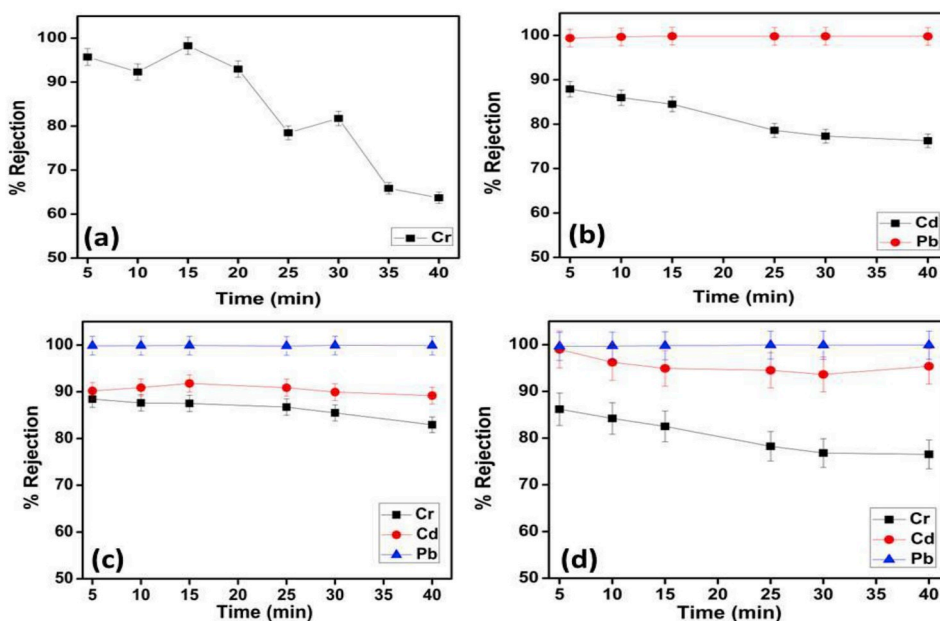

Fig. 7. Performance of fabricated membranes in separation of heavy metal ions: (a) FeS/PVDF membrane (b) CFFO/PVDF membrane (c) FeS/CFFO/PVDF membrane in acidic pH (d) Fes/CFFO/PVDF membrane in neutral pH.
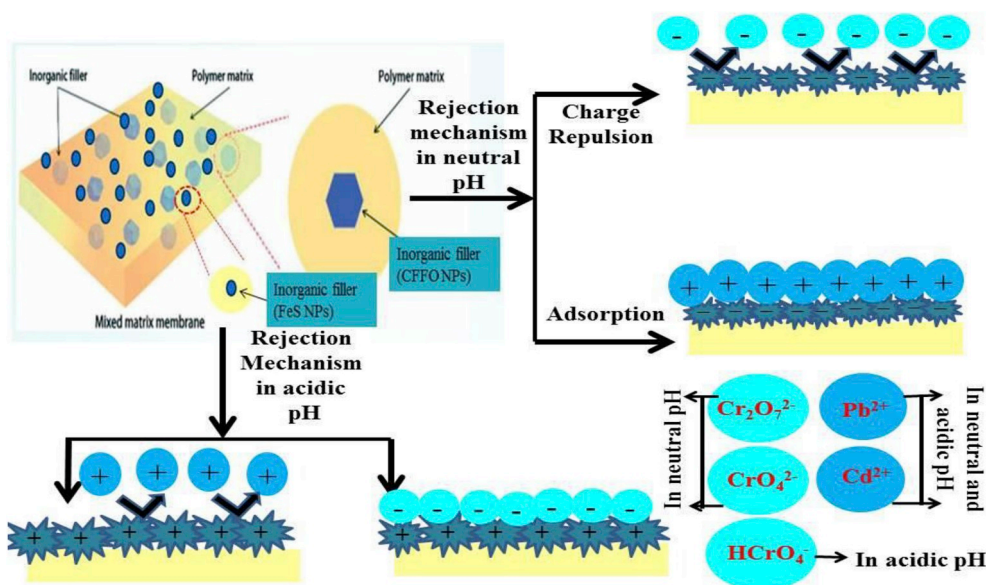
Fig. 8. Metal ion separation schematic diagram of FeS/CFFO/PVDF membrane.

Table 4

Adsorption isotherm parameters and correlation coefficients for multiple heavy metals adsorption on FeS/CFFO/PVDF membrane.

Heavy metal ions	Langmuir Model			Freundlich Model		
	q_{max} (mg/g)	b (ml/mg)	R^2	n	K_f ((mg/g) (L/mg)$^{1/n}$)	R^2
Cr	15.32	0.4329	0.932	1.94	1.318	0.985
Cd	20.40	0.1950	0.901	1.15	1.511	0.953
Pb	55.56	0.0142	0.946	1.10	2.65	0.912

Adsorption isotherm parameters and correlation coefficients for multiple heavy metals adsorption on FeS/CFFO/PVDF membrane are depicted in Table 4 and Fig. S8(SI).

3.4. Mechanism of interaction between fabricated membranes and the metal ions using XPS and FTIR studies

To study the interaction of Cr(VI), $Cd^{2+,}$ and Pb^{2+} with fabricated membranes, XPS and FTIR spectra were recorded. Fig. S9 (SI) illustrates the FTIR spectra of fabricated membranes after treatment of Cr(VI), Cd^{2+} and Pb^{2+} ions from their respective membranes. It is evident from the spectra of FeS/PVDF-Cr, a characteristic peak at 975 cm^{-1}, attributed to the stretching vibrations of Cr–O and Cr=O, confirms the adsorption of Cr(VI) on membrane surface [53]. However, in the spectra of CFFO/PVDF-Cd, a shift in –OH, –C=O, and –C-OH vibration band was observed and compared with the spectra of CFFO/PVDF (Fig. 5). The magnitude of frequency shifts attributed to the electrostatic attraction and chelation between Cd^{2+} and CFFO/PVDF [24]. Further, an additional vibrations occurred at 875 cm^{-1} and 769 cm^{-1} which could be assigned to the stretching frequency of Pb–O and Pb=O bond respectively. This indicates CFFO/PVDF is also proficient to interact with Pb^{2+} [24,30]. Besides, after Cr(VI), Cd^{2+} and Pb^{2+} treatment, some peaks in the spectrum of FeS/CFFO/PVDF-Cr-Cd-Pb slightly blue shifted, and some new peak was found at 974 cm^{-1} for the Cr=O stretching vibrations, 600-800 cm^{-1} for –Pb-O stretching vibration, which was probably attributed to the electrostatic interaction and chelation between multiple metal ions and FeS/CFFO/PVDF [23,53].

To further explore the interaction between FeS/CFFO/PVDF membrane and multiple metals ions (Cr(VI), Pb^{2+}, and Cd^{2+}) at molecular level, XPS spectra was recorded. Fig. S10(a) (SI) depicts the survey scan

spectrum of FeS/CFFO/PVDF membrane before and after treatment of multiple metal ions. It is evident that C 1s, O 1s, S 2p, Fe 2p, Cr 2p, Cd 3d and Pb 4f are identified. Thus the interaction of Cr(VI), Pb^{2+}, and Cd^{2+} onto FeS/CFFO/PVDF is validated and evident from the appearance of double peaks of Cr $2p_{3/2}$ and Cr $2p_{1/2}$, double peaks of Cd $3d_{5/2}$, Cd $3d_{3/2}$ and Pb $4f_{7/2}$ and Pb $4f_{5/2}$ in core level spectra (Fig. 9(a)-(c)). To get a further insight into the interaction of ions, the core level scans for C 1s, Fe 2p, S 2p, Cr 2p, Pb 4f, and Cd 3d on FeS/CFFO/PVDF before and after the treatment (denoted as FeS/CFFO/PVDF-Cr-Cd-Pb) were analyzed and molecular level peak fitting results are listed in Table S4 (SI). Two main peaks $2p_{1/2}$ and $2p_{3/2}$ at binding energies 582 and 578 eV, respectively, were observed in the core level spectra of Cr 2P (Fig. 9(a)). Additionally, splitting of multiple peaks are observed for the $2p_{3/2}$ peak. This suggests the reduction of Cr(VI) to Cr(III) from FeS NPs (Fe^{2+} and S^{2-} played key role in the reduction of Cr(VI)). Moreover, Fig. 9 (b) shows the molecular level Cd 3d spectrum, convolution of the Cd $3d_{5/2}$ and Cd $3d_{3/2}$ which could attribute to the formation of monodentate and bidentate complexes of Cd with active binding sites present on CFFO NPs. Besides, Pb 4f core level spectrum, further shows two peaks at 140 and 142 eV which indicated Pb^{2+} adsorption onto FeS/CFFO/PVDF occurred by the complexation of oxygen-containing functional groups (Fig. 9 (c).

Based on the above discussions of the FTIR and XPS studies, reaction scheme has also been suggested in Fig. S10 (SI) depicting the interaction between metal ions and active binding sites present on membrane.

3.5. Application of FeS/CFFO/PVDF membrane in real ground water treatment

3.5.1. Performance evaluation of FeS/CFFO/PVDF membrane for simultaneous removal of hazardous multiple heavy metal ions from real ground water samples of industrial areas

Generally, heavy metal ions tend to exist together in real ground water [54], thus simultaneous separation of multiple ions should be significant factor for consideration. Thus, in order to investigate the water treatment application of the developed FeS/CFFO/PVDF membrane for simultaneous removal of multiple heavy metal ions from real contaminated water, (complex water matrix), groundwater samples from industrial area were used as a feed solution. The concentration of heavy metal ions in collected groundwater samples were analyzed and results are presented in Table S5(SI).
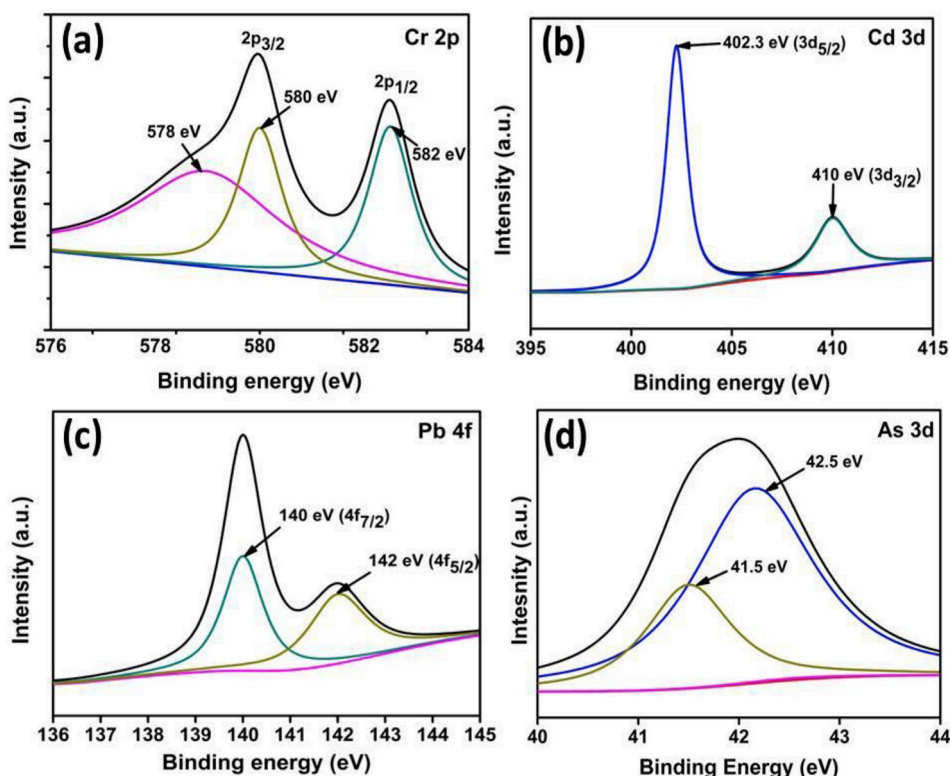
Fig. 9. Curve fitted high resolution scans of FeS/CFFO/PVDF membrane after filtration of metal ions for **(a)** Cr 2p **(b)** Cd 3d **(c)** Pb 4f **(d)** As 3d.
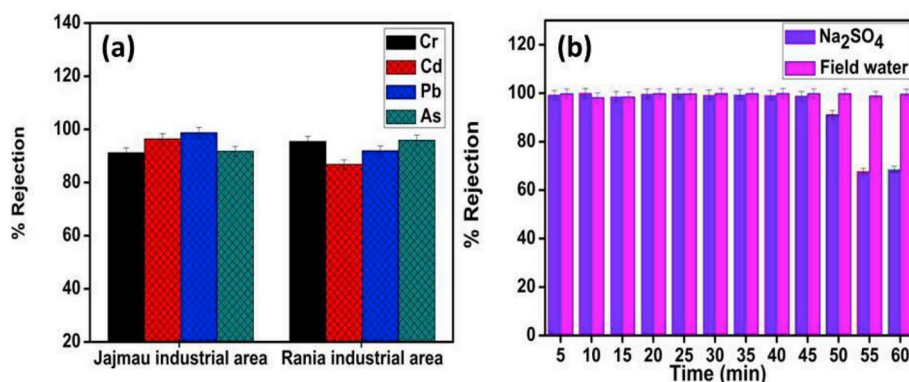

Fig. 10. (a) Metal ion rejection performance of FeS/CFFO/PVDF for real ground water treatment **(b)** Salt rejection performance of FeS/CFFO/PVDF and its application in real water sample.

To evaluate the performance of FeS/CFFO/PVDF, filtration experiments were performed. A final concentration of each metal ion after single filtration within 5 minutes is presented in Table S5 (SI). Fig. 10(a) shows percentage removal of each metal ions present in both samples of real ground water. It is evident from the results that FeS/CFFO/PVDF membrane showed outstanding performance towards simultaneous removal of toxic heavy metal ions, present in real ground water samples. The results indicated 91.2% and 95.4% removal of total Cr from Jajmau and Rania industrial area, respectively. On the other hand, 96.4% and 86.8% removal of Cd^{2+} from Jajmau and Rania industrial area, respectively was observed. In addition to this, pre-eminent rejection efficiency of 98.7% and 91.9% towards Pb^{2+} removal from Jajmau and Rania industrial area were observed.

Furthermore, one of the most exciting observation was detected in the case of total As removal. However, this developed membrane was tested in this study for the simultaneous separation of Cr, Cd, and Pb, but it is evident from the data (Tables S5 and SI), that developed membrane also exhibited excellent removal potential to separate total

As from real ground water samples with good rejection efficiency (91.7–95.9%). To investigate potential mechanism for As under the studied condition, we performed FTIR and XPS analysis with the specimen of used FeS/CFFO/PVDF membrane after the filtration of ground water samples. As shown in Fig. 9 (d), As 3d spectrum was observed which can be deconvulated into binding energy peaks at 44.2 and 41.5 eV, attributed to the AS(III) and As (V), respectively. The area percentage of As (III) was 196% of the total As area while As (V) was up to 75.5% suggesting transformation of As(III) to As(V) during the filtration process. Moreover, proficiency of this membrane was also verified by FTIR analysis. A new peak at 761 cm^{-1} was observed, corresponding to the As–O stretching vibration in the spectra of FeS/CFFO/PVDF-Cr-Cd-Pb-As (Fig. S9 (SI)).

Combination of above discussed results proves that FeS/CFFO/PVDF membrane is highly potent material to remove multiple metals ions simultaneously from ground water and bringing down the concentration of multiple metal ions to WHO limits.

3.5.2. Performance evaluation of the FeS/CFFO/PVDF membrane for the salt rejection from real water

The salt rejection efficiency of the FeS/CFFO/PVDF membrane with respect to the sulfate ion (SO_4^{2-}) was examined in the tap water of Indian Institute of Technology, Kanpur. The results of the study are presented in Fig. 10(b). Size exclusion (steric effects) and Donnan exclusion (electric repulsion) are two main factor which affect the rejection of salt [55,56]. The high rejection rate of sulfate ion through the membrane is due to the negatively charged surface which increases the charge-charge repulsion between the membrane surface and SO_4^{2-} ions. Moreover, the presence of FeS NPs in the membrane provides more accessible active binding sites in which sulfate ion adsorb, leads to an improved rejection. Beside this, highly hydrophilic nature of membrane reduces the formation of the polarized layer on the membrane surface which declines the salt percolation through the membrane and improves the salt rejection [40].

Applicability of the FeS/CFFO/PVDF membrane was examined in the real water samples. The initial conductivity of the real tap water sample was checked and found the value of 1678 µS/cm. Consequently, filtration of sample was done through FeS/CFFO/PVDF membrane and permeate of sample was collected at 5 min time intervals and observed that membrane exhibit the potential to reduce the conductivity from 1678 µS/cm to 3.9–6.2 µS/cm within 5 min filtration and constant with respect to time. From the observed value, approximately 99.76–99.62% decrease in conductivity was measured (Fig. 10(b)). These observed values were under the range of 200–800 µS/cm, set for drinking water according to Central pollution control board (CBCB) [48]. These exciting findings illustrated that developed FeS/CFFO/PVDF membrane, formed by the combination of NPs is exceptionally effective for the potential salt rejection from synthetic solution as well as in real water samples at the low pressure of 1 bar.

3.6. Comparison of performances with other membranes

A literature review on MMMs prepared with various compositions is depicted in Table 5. It can be observed from this table that main research focus has been concentrated on filtration of single heavy metal ions from synthetic water. However, only few studies are available on simultaneous removal of multiple heavy metal ions, but seldom any reports found on the applicability of membranes in real ground water treatment. Therefore, the membrane developed in this study can have potential application in ground water treatment, where multiple heavy metals can be found along with salts. Combined separation of multiple heavy metals ions and salts in a single step with high permeability, good mechanical and thermal stability and low pressure requirement offers a promising approach for the treatment of real life complex effluent.

3.7. Conclusion and future prospects

Two types of inorganic fillers, i.e. FeS and CFFO, were incorporated into PVDF matrix individually and combinedly, to prepare three different types of MMMs (FeS/PVDF, CFFO/PVDF, FeS/CFFO/PVDF). This work demonstrates preparation, characterization and application (specially FeS/CFFO/PVDF membrane for application) in purification of ground water samples contaminated with multiple heavy metal ions (Cr, Cd, Pb, As). Enhanced solvent-non solvent demixing made the membrane more porous leading to higher permeate flux. Characterization of NPs as well as their corresponding MMMs was done by various techniques to investigate the surface morphologies, chemical composition of NPs and MMMs, and uniform distribution of NPs on developed MMMs. In addition, evaluation of performance of developed membranes was done in terms of their porosity, water uptake capacity, hydrophilicity, permeation property, mechanical and thermal property and separation efficiency for multiple heavy metal ions removal, individually as well as simultaneously. The results of the study revealed

Table 5
Comparison of the performance of MMMs in heavy metals and salt contaminated water filtration.

Polymer	Nanofillers	Conc. Range (mg/L)/Operational pH	Heavy metal ions	Effective for Salt rejection	Treated water	Applicability in real water treatment	Ref.
PES	Fe$_3$O$_4$/GO	20/5	Cu^{2+}	–	Simulated water	NA	[57]
PES	Aminiated-TiO$_2$	10/acidic and basic	Cr(VI)	–	Simulated water	NA	[58]
PES	GO	1000/not mentioned	–	MgCl$_2$, NaCl, MgSO$_4$, Na$_2$SO$_4$	Simulated water	NA	[59]
PES	Al–TiO$_2$	10/not metioned	As(III), Cd^{2+}, Pb^{2+}	NA	Simulated water	NA	[41]
PVDF	Cu NPs and CNTs	100/5.0–9.0	As (III)	NA	Simulated water	NA	[60]
PES	Al$_2$O$_3$	20	Cu^{2+}	NA	Simulated water	NA	[61]
CA	TiO$_2$	10/3.5	Cr(VI)	NA	Simulated Water	NA	[11]
PVC 4-amino benzoic acid	–	10/acidic and neutral pH	Cd^{2+}, Pb^{2+} Cr(VI)	NA	Simulated Water	NA	[35]
PES/PA	HNTs	4,8,11	–	Using MgSO$_4$, NaCl	Simulated Water	NA	[62]
PVDF	FeS + CFFO	5/acidic and neutral pH	Cd^{2+}, Pb^{2+} Cr(VI)	Using Na$_2$SO$_4$	Simulated water and ground water	Ground water industrial area, effective to reduce conc.to WHO limit.	This study

that developed membranes showed enhanced porosity, high water up-take capacity, high water flux, good mechanical and thermal stability, and good separation efficiency for heavy metals. However, FeS/CFFO/PVDF membrane was found to be optimum and improved properties than unmodified PVDF, FeS/PVDF and CFFO/PVDF membranes due to synergestic effect of both NPs.

Moreover, filtration performance with multiple metal ions were also investigated of developed MMMs. It was found that FeS/CFFO/PVDF showed best filtration performance for simultaneous removal of multiple metal ions. FTIR and XPS showed the high involvement of the functional groups of the NPs towards the interactions of multiple metals ions. Owing to the improved performance, it was also explored in real ground water samples of industrial area for simultaneous removal of multiple heavy metal ions (Cr, Cd, Pb and As). In addition, this membrane was also applied in the real water for desalination study. It is evident from the results that FeS/CFFO/PVDF membrane efficiently removed multiple heavy metal ions simultaneously from industrial ground water samples and bringing down the concentration of multiple metal ions to WHO limits with desalination efficiency. Regeneration and enhancement of lifetime of membrane are future prospective of this study.

It is envisaged, that considering the alarming heavy metals (Cr, Cd, Pb, As) contamination scenario of Kanpur and various regions of India, the present study can provide a viable technological solution in the effort for the simultaneous removal of multiple heavy metals ions of complex effluents present in environment, in view of more than 1000 million people are exposed to severe health risk.

Acknowledgements

Appendix A. Supplementary data

Supplementary data to this article can be found online at https://doi.org/10.1016/j.memsci.2019.117422.

References

[1] H. Gholami Derami, Q. Jiang, D. Ghim, S. Cao, Y.J. Chandar, J.J. Morrissey, Y.-S. Jun, S. Singamaneni, A robust and scalable polydopamine/bacterial nanocellulose hybrid membrane for efficient wastewater treatment, ACS Appl. Nano Mater. 2 (2019) 1092–1101.

[2] P.S. Kumar, K. Venkatesh, E.L. Gui, S. Jayaraman, G. Singh, G. Arthanareeswaran, Electrospun carbon nanofibers/TiO2-PAN hybrid membranes for effective removal of metal ions and cationic dye, Environ. Nanotechnol. Monit. Manage. 10 (2018) 366–376.

[3] D. Yang, L. Li, B. Chen, S. Shi, J. Nie, G. Ma, Functionalized chitosan electrospun nanofiber membranes for heavy-metal removal, Polymer 163 (2019) 74–85.

[4] C.-C. Ye, Q.-F. An, J.-K. Wu, F.-Y. Zhao, P.-Y. Zheng, N.-X. Wang, Nanofiltration membranes consisting of quaternized polyelectrolyte complex nanoparticles for heavy metal removal, Chem. Eng. J. 359 (2019) 994–1005.

[5] Y.-H. Li, Z. Di, J. Ding, D. Wu, Z. Luan, Y. Zhu, Adsorption thermodynamic, kinetic and desorption studies of Pb2+ on carbon nanotubes, Water Res. 39 (2005) 605–609.

[6] M. Kumar, R. Nagdev, R. Tripathi, V.B. Singh, P. Ranjan, M. Soheb, A.L. Ramanathan, Geospatial and multivariate analysis of trace metals in tubewell water using for drinking purpose in the upper Gangetic basin, India: heavy metal pollution index, Groundw Sustain. Dev. 8 (2019) 122–133.

[7] H. Luan, B. Teychene, H. Huang, Efficient removal of As(III) by Cu nanoparticles intercalated in carbon nanotube membranes for drinking water treatment, Chem. Eng. J. 355 (2019) 341–350.

[8] Z. Rahman, V.P. Singh, Assessment of heavy metal contamination and Hg-resistant bacteria in surface water from different regions of Delhi, India, Saudi J. Biol. Sci. 25 (2018) 1687–1695.

[9] J.S. Uppal, Q. Zheng, X.C. Le, Arsenic in drinking water- Recent examples and updates from Southeast Asia, Curr. Opin. Environ. Sci. Health 7 (2019) 126–135.

[10] J. Xiao, L. Wang, L. Deng, Z. Jin, Characteristics, sources, water quality and health risk assessment of trace elements in river water and well water in the Chinese Loess Plateau, Sci. Total Environ. 650 (2019) 2004–2012.

[11] K.A. Gebru, C. Das, Removal of chromium (VI) ions from aqueous solutions using amine-impregnated TiO2 nanoparticles modified cellulose acetate membranes, Chemosphere 191 (2018) 673–684.

[12] L. Yan, P. Li, W. Zhou, Z. Wang, X. Fan, M. Chen, Y. Fang, H. Liu, Shrimp shell-inspired antifouling chitin nanofibrous membrane for efficient oil/water emulsion separation with in situ removal of heavy metal ions, ACS Sustain. Chem. Eng. 7 (2019) 2064–2072.

[13] M.R. Esfahani, N. Koutahzadeh, A.R. Esfahani, M.D. Firouzjaei, B. Anderson, L. Peck, A novel gold nanocomposite membrane with enhanced permeation, rejection and self-cleaning ability, J. Membr. Sci. 573 (2019) 309–319.

[14] R. Mukherjee, P. Bhunia, S. De, Nanofiltration range desalination by high flux graphene oxide impregnated ultrafiltration hollow fiber mixed matrix membrane, J. Clean. Prod. 213 (2019) 393–405.

[15] P. Liu, X. Wang, J. Ma, H. Liu, P. Ning, Highly efficient immobilization of NZVI onto bio-inspired reagents functionalized polyacrylonitrile membrane for Cr(VI) reduction, Chemosphere 220 (2019) 1003–1013.

[16] X. Wang, T. Wang, J. Ma, H. Liu, P. Ning, Synthesis and characterization of a new hydrophilic boehmite-PVB/PVDF blended membrane supported nano zero-valent iron for removal of Cr(VI), Separ. Purif. Technol. 205 (2018) 74–83.

[17] A.M. Nasir, P.S. Goh, A.F. Ismail, Highly adsorptive polysulfone/hydrous iron-nickel-manganese (PSF/HINM) nanocomposite hollow fiber membrane for synergistic arsenic removal, Separ. Purif. Technol. 213 (2019) 162–175.

[18] S. Jamshidifard, S. Koushkbaghi, S. Hosseini, S. Rezaei, A. Karamipour, A. Jafari rad, M. Irani, Incorporation of UiO-66-NH2 MOF into the PAN/chitosan nanofibers for adsorption and membrane filtration of Pb(II), Cd(II) and Cr(VI) ions from aqueous solutions, J. Hazard Mater. 368 (2019) 10–20.

[19] A. Rezvani-Boroujeni, M. Javanbakht, M. Karimi, C. Shahrjerdi, B. Akbari-adergani, Immoblization of thiol-functionalized nanosilica on the surface of poly(ether sulfone) membranes for the removal of heavy-metal ions from industrial wastewater samples, Ind. Eng. Chem. Res. 54 (2015) 502–513.

[20] A. Gao, K. Xie, X. Song, K. Zhang, A. Hou, Removal of the heavy metal ions from aqueous solution using modified natural biomaterial membrane based on silk fibroin, Ecol. Eng. 99 (2017) 343–348.

[21] M.A. Barakat, New trends in removing heavy metals from industrial wastewater, Arab. J. Chem. 4 (2011) 361–377.

[22] S. Ayyaru, Y.-H. Ahn, Application of sulfonic acid group functionalized graphene oxide to improve hydrophilicity, permeability, and antifouling of PVDF nanocomposite ultrafiltration membranes, J. Membr. Sci. 525 (2017) 210–219.

[23] D. Wang, G. Zhang, Z. Dai, L. Zhou, P. Bian, K. Zheng, Z. Wu, D. Cai, Sandwich-like nanosystem for simultaneous removal of Cr(VI) and Cd(II) from water and soil, ACS Appl. Mater. Interfaces 10 (2018) 18316–18326.

[24] M. Kumar, Z. Gholamvand, A. Morrissey, K. Nolan, M. Ulbricht, J. Lawler, Preparation and characterization of low fouling novel hybrid ultrafiltration membranes based on the blends of GOTiO2 nanocomposite and polysulfone for humic acid removal, J. Membr. Sci. 506 (2016) 38–49.

[25] C.-V. Gherasim, P. Mikulasek, Influence of operating variables on the removal of heavy metal ions from aqueous solutions by nanofiltration, Desalination 343 (2014) 67–74.

[26] A. Tora, Y. Cengelolub, M. Ersoz, G. Arslan, Transport of chromium through cation-exchange membranesby Donnan dialysis in the presence of some metals of different valences, Desalination 170 (2004) 151–159.

[27] D. Paul, Research on heavy metal pollution of river Ganga: a review, Ann. Agrar. Sci. 15 (2017) 278–286.

[28] Y. Li, W. Wang, L. Zhou, Y. Liu, Z.A. Mirza, X. Lin, Remediation of hexavalent chromium spiked soil by using synthesized iron sulfide particles, Chemosphere 169 (2017) 131–138.

[29] Z. Du, Y. Zhang, Z. Li, H. Chen, Y. Wang, G. Wang, P. Zou, H. Chen, Y. Zhang, Facile one-pot fabrication of nano-Fe3O4/carboxyl-functionalized baker's yeast composites and their application in methylene blue dye adsorption, Appl. Surf. Sci. 392 (2017) 312–320.

[30] V. Madhavi, T.N.V.K.V. Prasad, G. Madhavi, Synthesis and spectral characterization of iron based micro and nanoparticles, Iran, J. Energy Environ. 4 (2013) 385–390.

[31] D. Wang, G. Zhang, L. Zhou, M. Wang, D. Cai, Z. Wu, Synthesis of a multifunctional graphene oxide-based magnetic nanocomposite for efficient removal of Cr(VI), Langmuir, 33, 7007-7014.

[32] J.M. S, V. Nayak, M. Padaki, R.G. Balakrishna, K. Soontarapa, Eco-friendly membrane process and product development for complete elimination of chromium toxicity in wastewater, J. Hazard Mater. 332 (2017) 112–123.

[33] V. Nayak, R. Geetha Balakrishna, M. Padaki, K. Soontarapa, Zwitterionic ultra-filtration membranes for as (V) rejection, Chem. Eng. J. 308 (2017) 347–358.

[34] C. Liu, W. Bi, D. Chen, S. Zhang, H. Mao, Positively charged nanofiltration membrane fabricated by poly(acid–base) complexing effect induced phase inversion method for heavy metal removal, Chin. J. Chem. Eng. 25 (2017) 1685–1694.

[35] V. Nayak, M.S. Jyothi, R.G. Balakrishna, M. Padaki, S. Deon, Novel modified poly vinyl chloride blend membranes for removal of heavy metals from mixed ion feed

sample, J. Hazard Mater. 331 (2017) 289–299.

[36] S. Zinadini, A.A. Zinatizadeh, M. Rahimi, V. Vatanpour, H. Zangeneh, M. Beygzadeh, Novel high flux antifouling nanofiltration membranes for dye removal containing carboxymethyl chitosan coated Fe3O4 nanoparticles, Desalination (2014) 145–154.

[37] G. Zeng, Y. He, Y. Zhan, L. Zhang, Y. Pan, C. Zhang, Z. Yu, Novel polyvinylidene fluoride nanofiltration membrane blended with functionalized halloysite nanotubes for dye and heavy metal ions removal, J. Hazard Mater. 317 (2016) 60–72.

[38] V. Vatanpour, M.E. Yekavalangi, M. Safarpour, Preparation and characterization of nanocomposite PVDF ultrafiltration membrane embedded with nanoporous SAPO-34 to improve permeability and antifouling performance, Separ. Purif. Technol. 163 (2016) 300–309.

[39] A. Rahimpour, S.S. Madaeni, S. Zereshki, Y. Mansourpanah, Preparation and characterization of modified nano-porous PVDF membrane with high antifouling property using UV photo-grafting, Appl. Surf. Sci. 255 (2009) 7455–7461.

[40] N. Ghaemi, S.S. Madaeni, P. Daraei, H. Rajabi, S. Zinadini, A. Alizadeh, R. Heydari, M. Beygzadeh, S. Ghouzivand, Polyethersulfone membrane enhanced with iron oxide nanoparticles for copper removal from water: application of new functionalized Fe3O4 nanoparticles, Chem. Eng. J. 263 (2015) 101–112.

[41] K. Sunil, G. Karunakaran, S. Yadav, M. Padaki, V. Zadorozhnyy, R.K. Pai, Al-Ti$_2$O$_6$ a mixed metal oxide based composite membrane: a unique membrane for removal of heavy metals, Chem. Eng. J. 348 (2018) 678–684.

[42] R.S. Hebbar, A.M. Isloor, K. Ananda, A.F. Ismail, Fabrication of polydopamine functionalized halloysite nanotube/polyetherimide membranes for heavy metal removal, J. Mater. Chem. 4 (2016) 764–774.

[43] S.K. Hubadillah, M.H.D. Othman, Z. Harun, A.F. Ismail, M.A. Rahman, J. Jaafar, A novel green ceramic hollow fiber membrane (CHFM) derived from rice husk ash as combined adsorbent-separator for efficient heavy metals removal, Ceram. Int. 43 (2017) 4716–4720.

[44] A. Karkooti, A.Z. Yazdi, P. Chen, A. McGregor, N. Nazemifard, M. Sadrzadeh, Development of advanced nanocomposite membranes using graphene nanoribbons and nanosheets for water treatment, J. Membr. Sci. 560 (2018) 97–107.

[45] M. Komarek, C.M. Koretsky, K.J. Stephen, D.S. Alessi, V. Chrastn, Competitive adsorption of Cd(II), Cr(VI), and Pb(II) onto nanomaghemite: a spectroscopic and modeling approach, Environ. Sci. Technol. 49 (2015) 12851–12859.

[46] S. Chowdhury, M.A.J. Mazumder, O. Al-Attas, T. Husain, Heavy metals in drinking water: occurrences, implications, and future needs in developing countries, Sci. Total Environ. 569–570 (2016) 476–488.

[47] W.-P. Zhu, J. Gao, S.-P. Sun, S. Zhang, T.-S. Chung, Poly(amidoamine) dendrimer (PAMAM) grafted on thin film composite (TFC) nanofiltration (NF) hollow fiber membranes for heavy metal removal, J. Membr. Sci. 487 (2015) 117–126.

[48] W.-P. Zhu, S.-P. Sun, J. Gao, F.-J. Fu, T.-S. Chung, Dual-layer polybenzimidazole/polyethersulfone (PBI/PES) nanofiltration (NF) hollow fiber membranes for heavy metals removal from wastewater, J. Membr. Sci. 456 (2014) 117–127.

[49] N. Abdali, A. Marjani, F. Heidary, M. Adimi, Fabrication of PVA coated PES/PVDF nanocomposite membranes embedded with in situ formed magnetite nanoparticles for removal of metal ions from aqueous solutions, New J. Chem. 41 (2017) 6405–6414.

[50] M.G. Kochameshki, A. Marjani, M. Mahmoudian, K. Farhadi, Grafting of diallyldimethylammonium chloride on graphene oxide by RAFT polymerization for modification of nanocomposite polysulfone membranes using in water treatment, Chem. Eng. J. 309 (2017) 206–221.

[51] C. Mbareck, Q.T. Nguyen, O.T. Alaoui, D. Barillier, Elaboration, characterization and application of polysulfone and polyacrylic acid blends as ultrafiltration membranes for removal of some heavy metals from water, J. Hazard Mater. 171 (2009) 93–101.

[52] K.Y. Wang, T.-S. Chung, Fabrication of polybenzimidazole (PBI) nanofiltration hollow fiber membranes for removal of chromate, J. Membr. Sci. 281 (2006) 307–315.

[53] A.G. Khiratkar, S. Senthil Kumar, P.R. Bhagat, Designing a sulphonic acid functionalized benzimidazolium based poly(ionic liquid) for efficient adsorption of hexavalent chromium, RSC Adv. 6 (2016) 37757–37764.

[54] M.A. Salam, G. Al-Zhrani, S.A. Kosa, Simultaneous removal of copper(II), lead(II), zinc(II) and cadmium(II) from aqueous solutions by multi-walled carbon nanotubes, Compt. Rendus Chem. 15 (2012) 398–408.

[55] M. Dalwani, N.E. Benes, G. Bargeman, D. Stamatialis, M. Wessling, Effect of pH on the performance of polyamide/polyacrylonitrile based thin film composite membranes, J. Membr. Sci. 372 (2011) 228–238.

[56] J. Miao, L.-C. Zhang, H. Lin, A novel kind of thin film composite nanofiltration membrane with sulfated chitosan as the active layer material, Chem. Eng. Sci. 87 (2013) 152–159.

[57] G. Abdi, A. Alizadeh, S. Zinadini, G. Moradi, Removal of dye and heavy metal ion using a novel synthetic polyethersulfone nanofiltration membrane modified by magnetic graphene oxide/metformin hybrid, J. Membr. Sci. 552 (2018) 226–335.

[58] M.S. Jyothi, V. Nayak, M. Padaki, R.G. Balakrishna, K. Soontarapa, Aminated polysulfone/TiO$_2$ composite membranes for an effective removal of Cr (VI), Chem. Eng. J. 283 (2016) 1494–1505.

[59] Xue Wang, Huixian Wang, Yuanming Wang, Jian Gao, Jindun Liu, Yatao Zhang, Hydrotalcite/graphene oxide hybrid nanosheets functionalized nanofiltration membrane for desalination, Desalination 451 (2019) 209–218.

[60] H. Luan, B. Teychene, H. Huang, Efficient removal of As(III) by Cu nanoparticles intercalated in carbon nanotube membranes for drinking water treatment, Chem. Eng. J. 355 (2019) 341–350.

[61] N. Ghaemi, A new approach to copper ion removal from water by polymeric nanocomposite membrane embedded with -alumina nanoparticles, Appl. Surf. Sci. 364 (2016) 221–228.

[62] O.-A. Turkan, F. Celebi, B. Keskin, M.-S. Oyku, M. Agtas, T. Turken, A. Tufani, D.Y. Imer, G.O. Ince, T.U. Demir, Y.Z. Menceloglu, S. Unal, I. Koyuncu, Fabrication and characterization of temperature and pH resistant thin film nanocomposite membranes embedded with halloysite nanotubes for dye rejection, Desalination 429 (2018) 20–32.

Further reading

[63] S. Mishra, J. Dwivedi, A. Kumar, N. Sankararamakrishnan, Studies on salophen anchored micro/meso porous activated carbon fibres for the removal of uranium, RSC Adv. 5 (2015) 33023–33036.